Journal of Inorganic and Organometallic Polymers and Materials (2018) 28:1953–1961
https://doi.org/10.1007/s10904-018-0858-z

Biofabrication of Au–Pt Nanoparticles Using *Asarum europaeum* Extract and Evaluation of Their Activity in Degradation of Organic Dyes

Renata Dobrucka[1]

Received: 8 February 2018 / Accepted: 20 April 2018 / Published online: 23 April 2018

Abstract
Nanomaterials have attracted much attention in the recent years. The biological synthesis of metal nanoparticles is an important area of research in nanotechnology. This work describes a biological method for the synthesis of Au–Pt nanoparticles using the aqueous extract of *Asarum europaeum*. The synthesized Au–Pt nanoparticles were characterized by UV–Vis, scanning electron microscopy (SEM) with EDS profile, Fourier transform infrared spectroscopy (FTIR), transmission electron microscopy (TEM) and atomic force microscopy (AFM). The applied methods made it possible to determine the presence of Au–Pt nanoparticles sized 5–6 nm. The EDS profile shows a gold and platinum signal confirming the formation of Au–Pt nanoparticles. The synthesized Au–Pt nanoparticles were used as a catalyst for the remediation of malachite green and methylene blue. Base on the obtained results, the Au–Pt nanoparticles synthesized using *Asarum europaeum* showed good catalytic activity in the reduction of methylene blue and malachite green.

Keywords Green synthesis · Au–Pt nanoparticles · Catalytic activity

1 Introduction

Metal nanoparticles exhibit completely new or improved properties with larger particles of the bulk materials, and these novel properties are derived due to the variation in specific characteristics, such as size, distribution and morphology of the particles. The noble metal nanoparticles, such as gold, silver or platinum, play an important role in numerous fields of science. A great emphasis is also put on multi-component metal nanoparticles, which are very useful in catalyst, sensor and medical applications. Multi-component metal nanoparticles usually provide novel or enhanced properties, which are not available from their individual components [1–3].

It is common knowledge that organic dyes are widely used in many branches of industry. Such dyes include malachite green oraz mehylene blue. Malachite green (MG) is a cationic dye that is widely used for the dyeing of silk, wool, jute, leather, paper, distilleries, as a food colouring agent, food additive, and in medical disinfectant and fish industries. According to Parshetti et al. [4] 10–15% of malachite green dyes are directly lost to wastewater in the process. Methylene blue is a cationic, toxic dye which can cause mutations, allergic dermatitis, cancer, skin irritation, eye burns in humans and animals, cyanosis, methemoglobinemia, convulsions, dyspnea and tachycardia [5, 6]. It has been observed that industrial dyeing sewages strongly alter the biological, chemical and physical feature of aquatic system through perpetual variations of temperature, odor, turbidity, noise etc., which is harmful to public health, fish, livestock, wildlife, and other biodiversity as well [7].

Most synthetic dyes are very resistant to biological degradation, heat, light as well as chemical and other oxidation compounds [8]. Also, researchers are stirring and trying their best to resolve these existing problems of environmental pollution properly by sanitizing the waste contaminated water [9]. Various chemical and physical treatment methods, such as coagulation, precipitation filtration, membrane separation, electrodialysis, biological treatment, oxidation and adsorption, have been used for the removal of dyes from wastewater [10]. The photocatalytic degradation of organic as well as inorganic dyes is a promising and ambitious technology, which has a strong effect on the removal of different dyes existing in wastewater [11]. It is well-known that the

✉ Renata Dobrucka
renata.dobrucka@ue.poznan.pl

[1] Department of Industrial Products Quality and Ecology, Faculty of Commodity Science, Poznan University of Economics, al. Niepodległości 10, 61-875 Poznan, Poland

size of metal nanoparticle plays an important role in catalytic reduction, and that nanoparticles exhibit size-dependent catalytic properties [12]. The nanostructured materials not only provide a specific surface area but also a more dispersed active site for the catalyst to provide excellent photocatalyst performance [13]. Besides, smaller nanoparticles show faster catalytic activity.

The nanoparticles of platinum and gold exhibit catalytic properties. According to the world literature, the catalytic activity of Au/Pt/Ag nanoparticles is higher than that of Au nanoparticles with nearly the same particle size. Also the studies conducted by Park et al. [14] demonstrated that the Pt-modified Au nanoparticles exhibited higher catalytic activity for methanol oxidation than pure Pt nanoparticles. Properties and particle size of the nano composites can be controlled by different synthesis methods [15, 16]. There are various methods for preparing Au–Pt nanoparticles; however, they are mainly chemical or physico–chemical. In the recent years, there has been a greater interest in the biological synthesis of nanoparticles. Researchers have tried to find biological methods for the synthesis of nanoparticles that will be an alternative to chemical or physical methods [17, 18]. Biological methods for the production of nanoparticles are considered safe and environmentally friendly; moreover, they are cost-effective and ensure the complete elimination of toxic chemicals [5].

This work used *Asarum europaeum. A. europaeum* is a perennial species that belongs to the Aristolochiaceae family. It grows in the fertile forests of Central and Southern Europe as well as in Siberia. The asarabacca herb contains 0.8–1% essential oil, tannins, resin, starch, saccharose, phenolic glycosides, and sesquiterpenes. Asarabacca also contains phytoncides with strong antimicrobial properties. In the essential oil, there can be found such substances as eugenol, asaron, l-pinen, methyl eugenol and acrolein. Due to the presence of numerous active substances, it was decided to use *A. europaeum* in order to obtain Au–Pt nanoparticles.

2 Experimental

2.1 Materials

All reagents: $HAuCl_4$, K_2PtCl_6 and organic dyes were purchased from Sigma-Aldrich (Poland, Poznan). Milli-Q water was used throughout the experiment.

2.2 Synthesis of Au–Pt Nanoparticles

Asarum europaeum was collected from Wielkopolska region (Poland). 2 g of powdered A. europaeum was put into 250 ml of an aqueous solution and ethanol in the 21 ratio. The solution was heated and stirred vigorously for 60 min at 85 °C. The obtained extract was used immediately after filtration through Whatman's No. 1 filter paper. Then, solution I was prepared. In order to prepare solution I, prepared extract was mixed with 1 mM of the aqueous solution of $HAuCl_4$ in the 1:1 ratio. Next, solution II was prepared by mixing 1 mM of K_2PtCl_6 with the extract in the 1:1 ratio. Both solutions were stirred for 12 h at 90 °C. After that time, solutions I and II were mixed in the 1:1 ratio. The obtained solution was stirred for 24 h at 80 °C. The absorbance readings were made 2, 4, 8 and 24 h after the combination of both solutions in order to check the progress of the reaction.

2.3 Characterization of Au–Pt Nanoparticles

The optical property of Au–Pt nanoparticles was analyzed via ultraviolet and visible absorption spectroscopy (spectrophotometer Cary E 500) in the range 300–800 nm. Do badania binding properties of Au–Pt nanoparticles Fourier transform infrared spectroscopy (FTIR) analysis was used. Analysis FTIR was conducted using Perkin Elmer Spectrum 1000, in attenuated total reflection mode and using spectral range of 4000–380 cm^{-1}, with a resolution of 4 cm^{-1}. The nanoparticles size was analyzed using high resolution scanning electron microscope (HR SEM) Helios NanoLab 660 (FEI) and the composition was investigated using energy-dispersive X-ray spectroscopy (EDX). The shape and size of the synthesized Au–Pt nanoparticles was analyzed using a transmission electron microscope (TEM) JEOL JEM 1200 EXII operating at accelerated voltage of 80 keV. Atomic force microscopy (AFM) was conducted INTEGRA SPECTRA SOLAR of NT-MDT brand, measurement tips dedicated for NSGO1 high-resolution measurements. The resonance frequency of the tips ranged from 87 to 230 kHz. The force constant ranged from 1.45 to 15.1 Nm^{-1}, and the scanning area was 10 µm × 10 µm. Within the scanning area, there were 1000 × 1000 scanning points.

2.4 Catalytic Properties of Au–Pt Nanoparticles

The catalytic activity of Au–Pt nanoparticles was evaluated using UV–Vis spectrophotometer Cary E 500 to monitor the absorbance peaks. The absorbance was measured in the range of 450–800 nm at room temperature. The study of the catalytic activity of Au–Pt nanoparticles was conducted with the use of the aqueous solution of methylene blue and malachite green (1×10^{-4}M). Firstly, the aqueous solution of methylene blue and malachite green was monitored by measuring the absorbance intensity. In the next step, 4 ml of methylene blue and malachite green, 0.5 ml of *A. europaeum* herb water extract and 3 ml of Milli Q water were analyzed. Then, the absorbance was measured for the solution containing 4 ml of organic dyes (1×10^{-4} M), 0.5 ml of *A. europaeum* herb water extract,

0.5 ml of the prepared solution of Au–Pt nanoparticles and 2.5 ml of Milli Q water. The absorbance was measured at 5-min intervals for 30 min. At that time, there was observed a reduction of the organic dyes: methylene blue and malachite green.

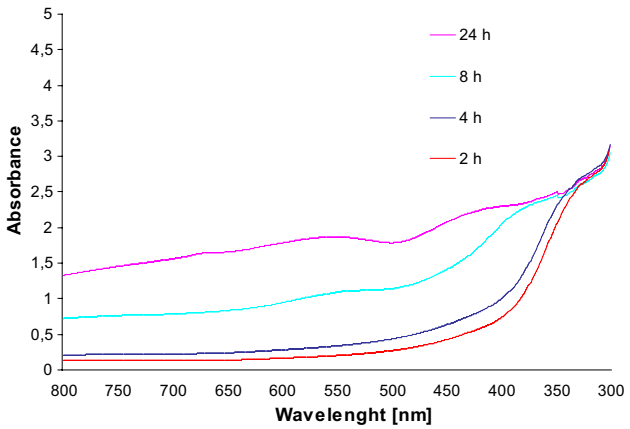

Fig. 1 UV–Visible spectra of synthesized Au–Pt nanoparticles using *A. europaeum*

3 Results and Discussion

3.1 UV–Visible Absorption

As it is known, UV–Vis spectroscopy is one of important techniques to determine the formation of metal nanoparticles in an aqueous solution. UV–Vis (ultraviolet and visible light) absorption spectra were measured over a range of 300–800 nm with spectrophotometer Cary E 500 using a quartz cell with 10 mm of optical path length. UV–Vis tool gave the absorbance of the Au–Pt nanoparticles. The absorbance was read 2, 4, 8 and 24 h after both solutions have been mixed. Figure 1 presents the UV–visible spectra of Au–Pt nanoparticles synthesized using *A. europaeum*. After 2 and 4 h, the peak was observed at 330 nm; it suggested the presence of Pt ions in the examined solution. Only after 24 h the peak at 330 nm indicated the presence of Pt°. The peak at 550 nm confirmed the presence of Au° in this solution.

3.2 FTIR Analysis

The FTIR measurement was carried out to identify the possible biomolecules responsible for the capping and efficient stabilization of the synthesized Au–Pt nanoparticles. Figure 2 presents the FTIR spectra of Au–Pt nanoparticles synthesized using Asarum europaeum. The spectra show bands at 3312, 2121, 1634, 390, 419 and 398 cm^{-1}. The strong

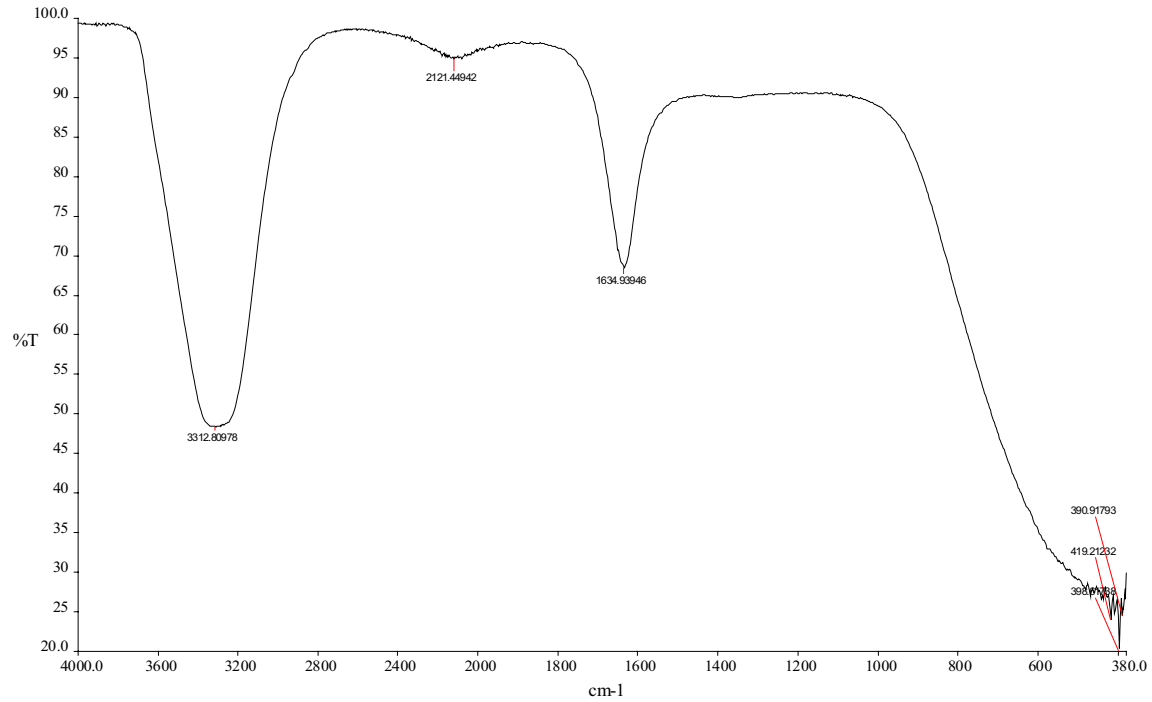

Fig. 2 FTIR spectrum of synthetised Au–Pt nanoparticles using *A. europaeum*

peak at 3312 cm^{-1} was observed for the O–H bond vibrations of the hydroxyl group. The band which appeared at 2121 cm^{-1} may indicate the presence of the alkynes group. The most intense band at 1634 cm^{-1} corresponds to amide bonds of proteins that may arise due to carboxyl stretching [6, 7]. The band at 390 and 398 cm^{-1} is attributed to the deformation vibration of C–C in polymer chains. The studies confirm the presence of active compounds that are found in *A. europaeum*. It has been assumed that the bioactive compounds act as the reducing and capping agents of Au–Pt nanoparticles. Phenolic compounds have good antioxidant proprieties; they inhibit the production of reactive oxygen species (ROS), and thus constitute a protection against oxidative stress [8]. Moreover, the number of hydroxyl groups and their location in a phenolic acid particle are responsible for the ability to neutralize radicals and prevent oxidation by natural phenolic compounds, such as caffeic acid. In the reactions with free radicals, –OH groups act as hydrogen donors, which leads to the emergence of phenoxyl radical. The presence of an –OH group in the ortho position significantly influences the increase in the antioxidant properties of phenolic acids [9]. Chlorogenic acid present in *A. europaeum* is highly effective in inhibiting the oxidation of LDL in vitro, which is comparable with the activity of caffeic acid [10, 11]. Figure 3 shows the chemical structure of active compounds present in *A. europaeum* : (A) Chlorogenic acid, (B) Caffeic acid, (C) Eugenol and (D) Asaron.

3.3 SEM and TEM Analysis

TEM is a well-established method for observing the sizes of nanoparticles. Figure 4 shows the TEM and SEM images of Au–Pt nanoparticles synthesized using *A. europaeum*. The TEM images (Fig. 8a the scale bar: 200 nm and b 100 nm) confirmed that the size of the synthesized Au–Pt nanoparticles was about 5 nm. Moreover, transmission electron microscopy (TEM) images present very small irregular nanoparticles of Au–Pt. The morphology of the synthesized Au–Pt nanoparticles was studied using scanning electron microscopy (SEM). Figure 5c, d present the SEM images of Au–Pt nanoparticles at different magnifications (respectively ×50,000 and ×300,000). The size

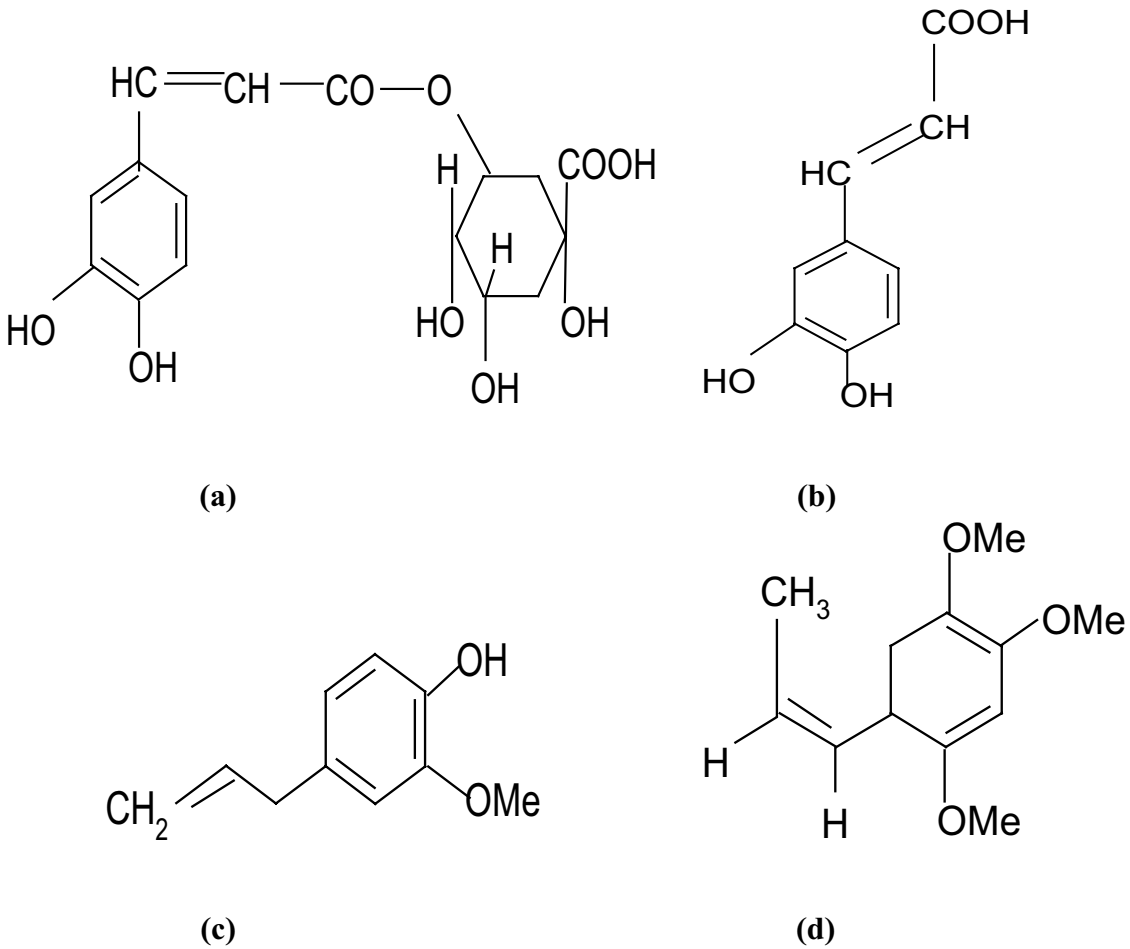

Fig. 3 The chemical structure of active compounds present in *A. europaeum*: **a** Chlorogenic acid, **b** Caffeic acid, **c** Eugenol and **d** Asaron

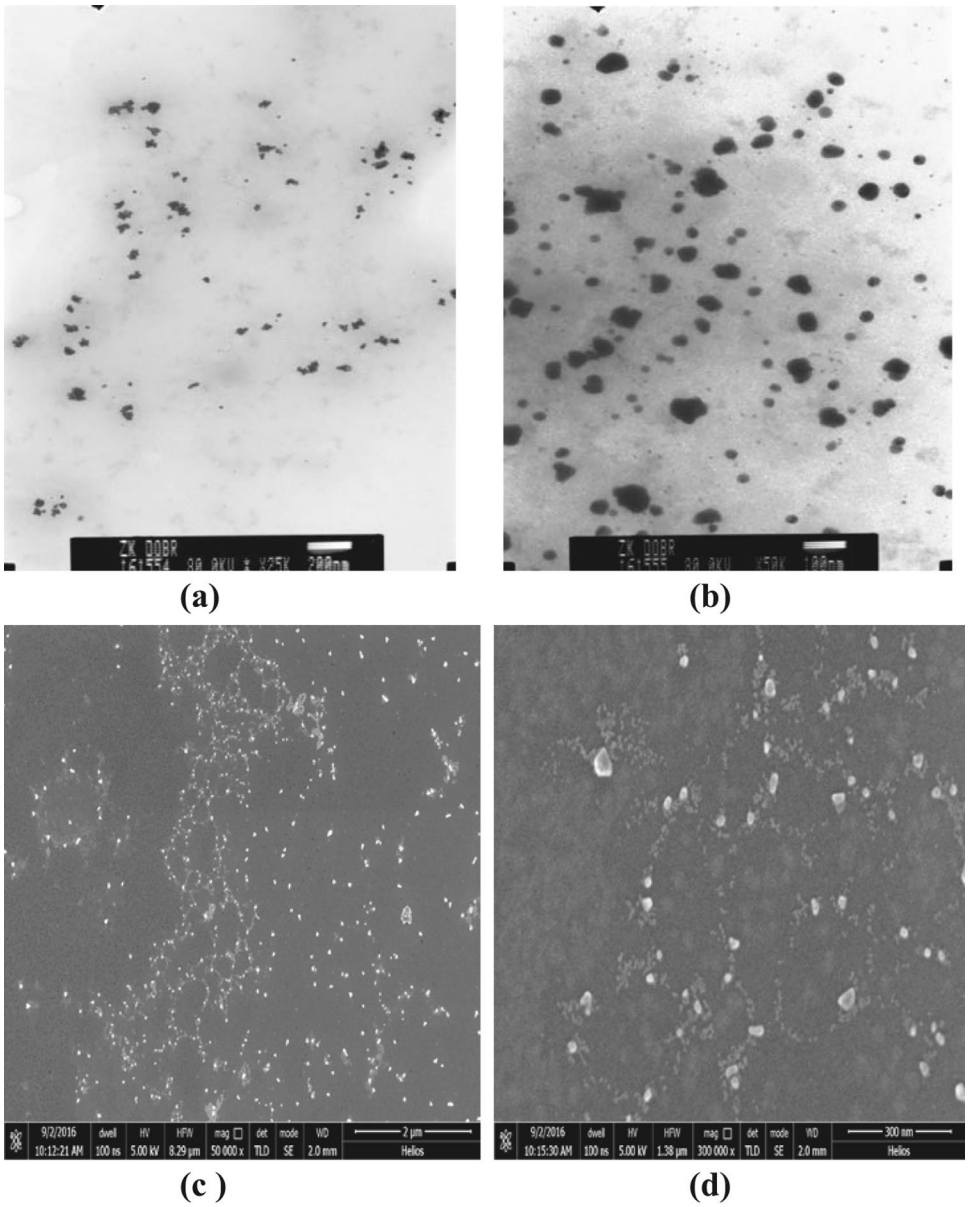

Fig. 4 TEM and SEM images of synthesized Au–Pt nanoparticles using *A. europaeum*, the scale bar **a** 200 nm, **b** 100 nm, magnificaton **c** ×50,000 and **d** ×300,000

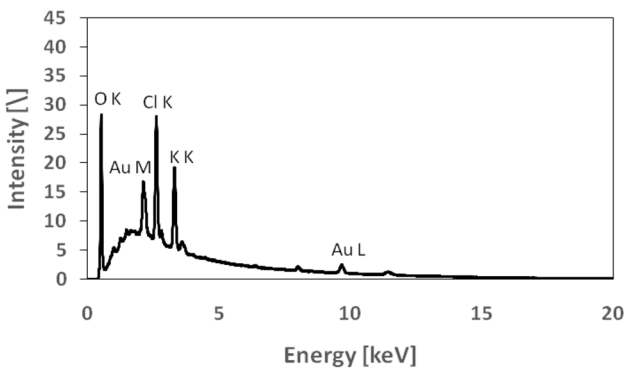

Fig. 5 EDS spectra of synthesized Au–Pt nanoparticles using *A. europaeum*

of very small synthesized Au–Pt nanoparticles was about 5–6 nm. In places, the bigger nanoparticles are visible. It is a effect of places of agglomeration of nanoparticles.

3.4 EDS Profile

Figure 5 presents the EDS spectra of Au–Pt nanoparticles synthesized using *A. europaeum*. The EDS profile shows a gold and platinum signal confirming the formation of Au–Pt nanoparticles. The EDS profile is the additional evidence of the formation of Au–Pt nanoparticles.

3.5 AFM Analysis

The analysis of the size of the Au–Pt nanoparticles synthesized using *A.europaeum* was performed by means of the atomic force microscopy (AFM). The size of the studied nanopartciles was about 5 nm. They also showed considerable stability. This study confirmed the previous results (SEM and TEM), which also indicated that the size of the Au–Pt nanoparticles was about 5 nm. Figure 6 shows AFM image of the synthesized Au–Pt nanoparticles using *A. europaeum* where: (a) the topography 10 µm × 10 µm, (b) the topography 10 µm × 10 µm with selected section, (c) the topography 3 µm × 3 µm, (d) the topography 1.5 µm × 1.5 µm.

3.6 Catalytic Activity of Au–Pt Nanoparticles

In this work, the synthesized Au–Pt nanoparticles were used as a catalyst for the remediation of malachite green and methylene blue. The first step of the experiment was to measure the absorbance of the aqueous solutions of methylene blue and malachite green. Then, the examined dye, the aqueous solution and distilled water were mixed. The obtained solution was examined for the period from 5 to 30 min. The absorbance was measured at 5-min intervals.

Figure 7 presents UV–Vis absorption spectra of the malachite green reduction by Au–Pt nanoparticles synthesized using *A. europaeum* extract for a time period of 30 min. The maximum absorbance value of malachite green was recorded at 615 nm. During 30 min of exposure to UV–VIS

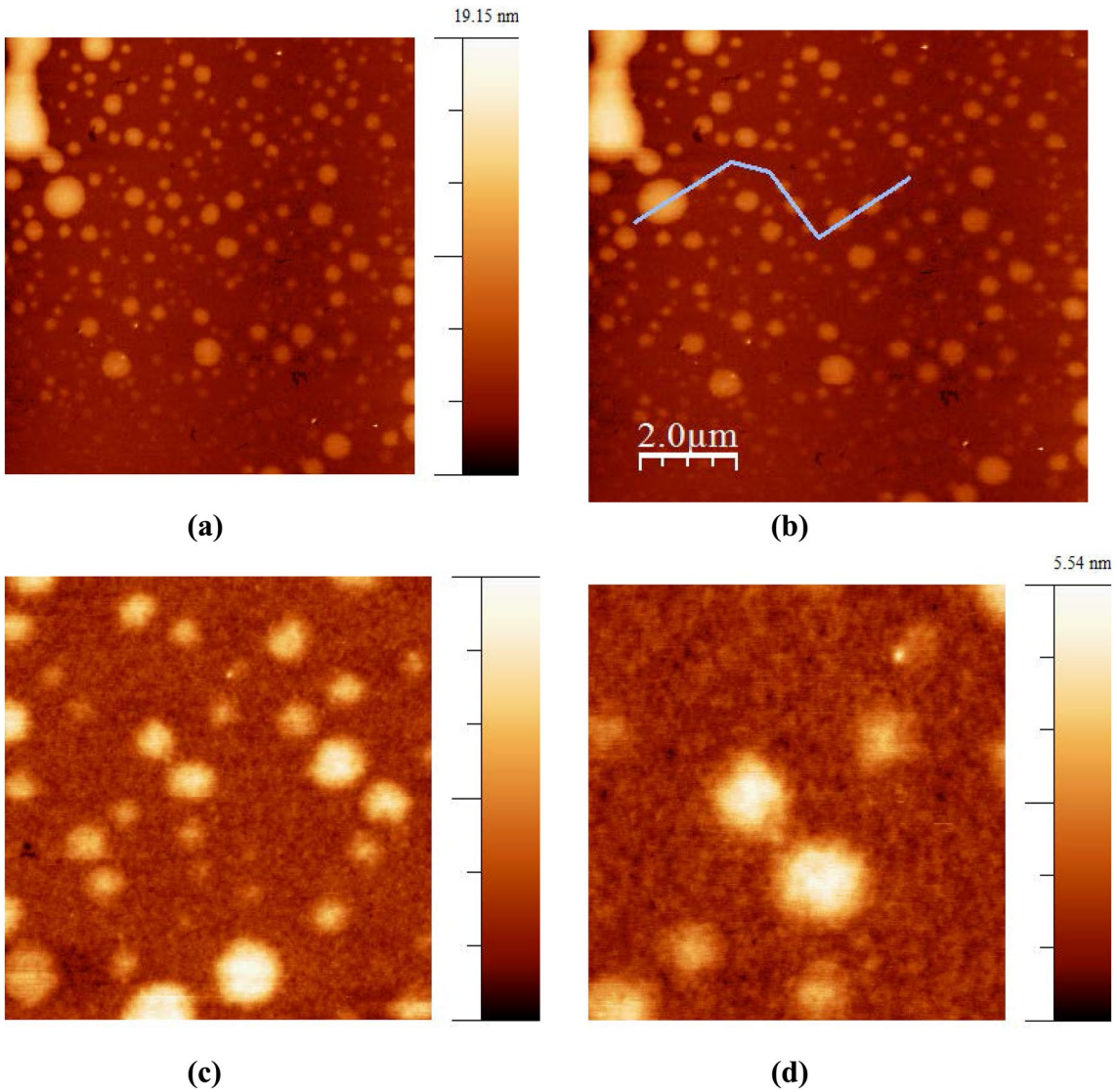

Fig. 6 AFM image of the synthesized Au–Pt nanoparticles using *A. europaeum* **a** the topography 10 µm × 10 µm, **b** the topography 10 µm × 10 µm with selected section, **c** the topography 3 µm × 3 µm, **d** the topography 1.5 µm × 1.5 µm

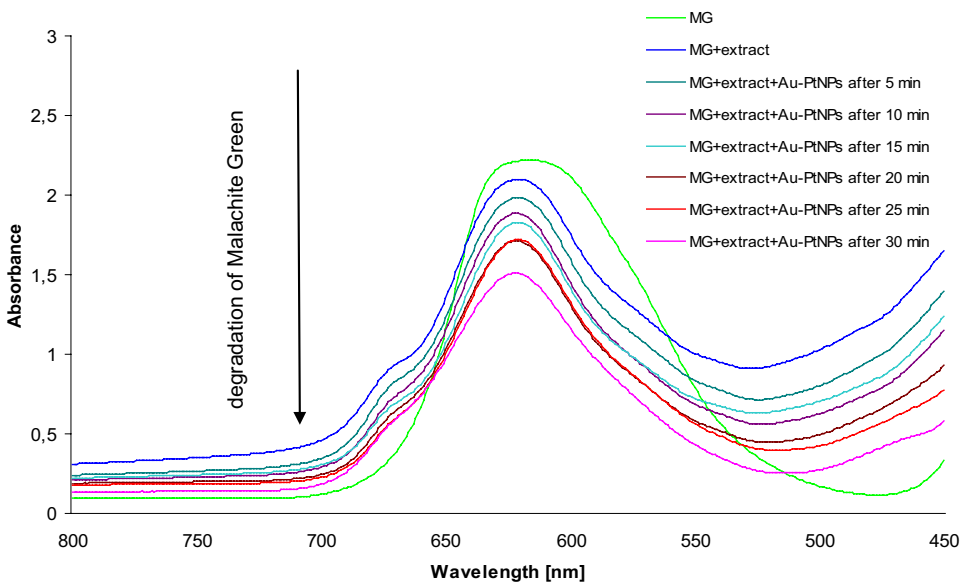

Fig. 7 UV–Vis absorption spectra of malachite green reduction by Au–Pt nanoparticles synthesized using *A. europaeum* extract. (Color figure online)

radiation, it was observed that the absorbance intensity peak of malachite green reduction decreased quickly and shifted to higher wavelength side. This diagram shows the degradation of malachite green with the use of Au–Pt nanoparticles synthesized using *A. europaeum* extract.

Figure 8 shows UV–Vis absorption spectra of methylene blue reduction by Au–Pt nanoparticles synthesized using *A. europaeum* extract for a time period of 30 min. The degradation of methylene blue is clearly visible. The maximum absorbance value of methylene blue was recorded at 660 nm. After 30 min, there was observed a significant decrease of methylene blue. In addition, the color changed from intense blue to light blue.

These studies show that Au–Pt nanoparticles synthetized biologically, using *A.europaeum*, exhibited high catalytic activity. According to Aswathy Aromal et al. [19], the speed of the reduction increases when the size of nanoparticles decreases. In accordance with this theory, the small size of the obtained Au–Pt nanoparticles contributed to their high efficiency in the reduction of organic dyes, as smaller

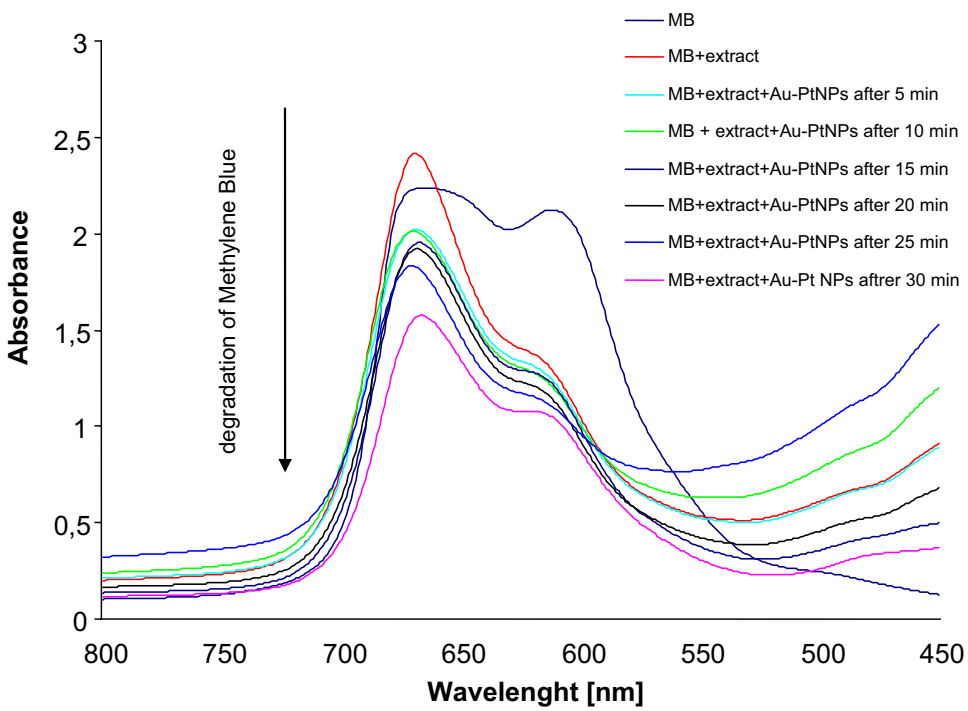

Fig. 8 UV–Vis absorption spectra of methylene blue reduction by Au–Pt nanoparticles synthesized using *A.europaeum* extract. (Color figure online)

nanoparticles show faster activity. The catalytic activity of Au [19] or Pt [8] has been discussed by many authors. However, the multi-component nanoparticles show greater catalytic properties than individual metal nanoparticles. Zhang and Toshima reported that the catalytic activity of Au/Pt/Ag nanoparticles is higher than that of Au nanoparticles with nearly the same particle size [20].

Titanium dioxide (TiO_2) is one of the best material due to excellent properties such as nontoxicity, strong oxidizing power and stability [21]. Zhou et al. [22] showed the activity of gold supported on mesoporous TiO_2 in the degradation process of Rhodamine-B. The Au–TiO_2 presented the highest visible activity due to the synergistic effect of gold nanoparticles and the improved efficiency of the interfacial charge transfer proces. Hai et al. showed that titania surface modification with Au, Cu and bimetallic Au–Cu NPs enables the increase of the photocatalytic activity under UV–visible irradiation [23]. Tabatabaei et al. [24] found that Au–TiO_2 exhibited the best photocatalytic activity in the degradation of methylene blue in the presence of visible light irradiation. Reedy et al. [25] founded that the heterogeneous Ag–TiO_2 composite showed a higher activity than the pure TiO_2 nanofiber. The enhanced activity can be attributed to the excellent distribution and interaction of Ag nanoparticles with the TiO_2 nanofiber support also, current studies prove that the application of two components of metal nanoparticles gives great effects in the degradation of organic dyes. This is a proposal solution used in the degradation of organic dyes.

4 Conclusion

Metal nanoparticles have come into focus due to their wide and highly interesting properties. Green synthesized metal nanoparticles have gained considerable attention in the recent years as a result of their potential applications in various fields of science. One of such interesting applications is the degradation of dyes. This work presents the biological method for synthesizing multi-component Au–Pt nanoparticles with the use of *A. europaeum* extract. The examination methods used in the work, i.e. UV–Vis, SEM, TEM, FTIR and AFM, made it possible to characterize the obtained nanoparticles in detail. The applied methods confirmed that the size of the nanoparticles was about 5–6 nm. The EDS profile provided the additional evidence of the formation of Au–Pt nanoparticles. The synthesized Au–Pt nanoparticles were used as a catalyst for the remediation of malachite green and methylene blue. The catalytic activity of Au–Pt nanoparticles was evaluated using UV–Vis spectrophotometer Cary E 500 to monitor the absorbance peaks. The absorbance was measured at 5-min intervals for 30 min. There has been observed an efficient degradation of malachite green and methylene blue in the presence of the obtained Au–Pt nanoparticles. The prepared Au–Pt nanoparticles showed very good catalytic activity. This work is anticipated to open new directions in the synthesis of multi-component Au–Pt nanoparticles which are highly efficient in the removal of organic dyes.

Acknowledgements This work has been financed from grant for young researchers in 2016 of the Ministry of Science and Higher Education.

References

1. C.J. Zhong, J. Luo, B. Fang, B.N. Wanjala, P.N. Njoki, R. Loukrakpam, J. Yin, Nanotechnology **21**(6), 062001 (2010)
2. L. Feng, G. Gao, P. Huang, K. Wang, X. Wang, T. Luo, C. Zhang, Nano Biomed. Eng. **2**(4), 258–267 (2010)
3. Y.P. Zhang, S.H. Lee, K.R. Reddy, A.I. Gopalan, K.P. Lee, J. Appl. Polym. Sci. **104**(4), 2743–2750 (2007)
4. G. Parshetti, S. Kalme, G. Saratale, S. Govindwar, Biodegradation of malachite green by Kocuriarosea MTCC1532. Acta Chim. Slov. **53**, 492–498 (2006)
5. A.M. Vargas, A.L. Cazetta, M.H. Kunita, T.L. Silva, V.C. Almeida, Chem. Eng. J. **168**, 722–730 (2011)
6. M.S. Ur Rehman, I. Kim, J.I. Han, Carbohydr. Polym. **90**, 1314–1322 (2012)
7. M.B. Tahir, G. Nabi, N.R. Khalid, M. Rafique, Ceram. Int. (2017). https://doi.org/10.1016/j.ceramint.2017.12.223
8. K.A. Adegoke, O.S. Bello, Dye sequestration using agricultural wastes as adsorbents. Water Resour. Ind. **12**, 8–24 (2015)
9. M.B. Tahir, G. Nabi, T. Iqbal, M. Sagir, M. Rafique, Ceram. Int. (2018). https://doi.org/10.1016/j.ceramint.2018.01.081
10. S. Agarwal, I. Tyagi, V.K. Gupta, S. Mashhadi, M. Ghasemi, J. Mol. Liq. **223**, 1340–1347 (2016)
11. M.B. Tahir, M. Sagir, M. Zubair, M. Rafique, I. Abbas, M. Shakil, A. Ahmed, J. Inorg. Organomet. Polym Mater. (2017). https://doi.org/10.1007/s10904-017-0771-x
12. K.R. Reddy, B.C. Sin, C.H. Yoo, W. Park, K.S. Ryu, J.S. Lee, Y. Lee, Scr. Mater. **58**(11), 1010–1013 (2008)
13. M.B. Tahir, G. Nabi, N.R. Khalid, W.S. Khan, J. Inorg. Organomet. Polym Mater. (2017). https://doi.org/10.1007/s10904-017-0714-6
14. I.S. Park, K.S. Lee, D.S. Jung, H.Y. Park, Y.E. Sung, Electrochim. Acta **52**, 5599 (2007)
15. M.B. Tahir, T. Iqbal, A. Hassan, S. Ghazal, J. Inorg. Organomet. Polym Mater. **27**(5), 1430–1438 (2017)
16. M. Parishani, M. Nadafan, Z. Dehghani, R. Malekfar, G.H.H. Khorrami, Result Phys. **7**, 3619–3623 (2017)
17. X. Deng, C.K. Chan, H. Tüysüz, ACS Appl. Mater. Interfaces **8**(47), 32488–32495 (2016)
18. G. Parshetti, S. Kalme, G. Saratale, S. Govindwar, Acta Chim. Slov. **53**, 492–498 (2006)
19. S.A. Aromal, K.D. Babu, D. Philip, Spectrochim. Acta A **96**, 1025–1030 (2012)
20. H. Zhang, N. Toshima, Appl. Catal. A **400**, 9 (2011)
21. N.R. Khalid, M. Liaqat, M.B. Tahir, G. Nabi, T. Iqbal, N.A. Niaz, Ceram. Int. **44**(1), 546–549 (2018)
22. M. Zhou, J. Zhang, B. Cheng, H. Yu, Int. J. Photoenergy (2012). https://doi.org/10.1155/2012/532843

23. Z. Hai, N. El Kolli, D.B. Uribe, P. Beaunier, M. José-Yacaman, J. Vigneron, H. Remita, J. Mater. Chem. A **1**(36), 10829–10835 (2013)
24. S.M. Tabatabaei, M.E. Boushehri, S. Yavari, J. Basic Appl. Sci. Res. **2**(8), 7459–7465 (2012)
25. K.R. Reddy, K. Nakata, T. Ochiai, T. Murakami, D.A. Tryk, A. Fujishima, J. Nanosci. Nanotechnol. **11**(4), 3692–3695 (2011)